Search for Higgs boson pair production in $\gamma\gamma$bb final state in pp collisions at $\sqrt{s}$ = 13 TeV with the ATLAS detector

Zihang Jia[1,2]

[1]IHEP, [2]Nanjing University

Outline

Motivation

Analysis overview

Categorization

Signal and backgound modeling

Results

Summary

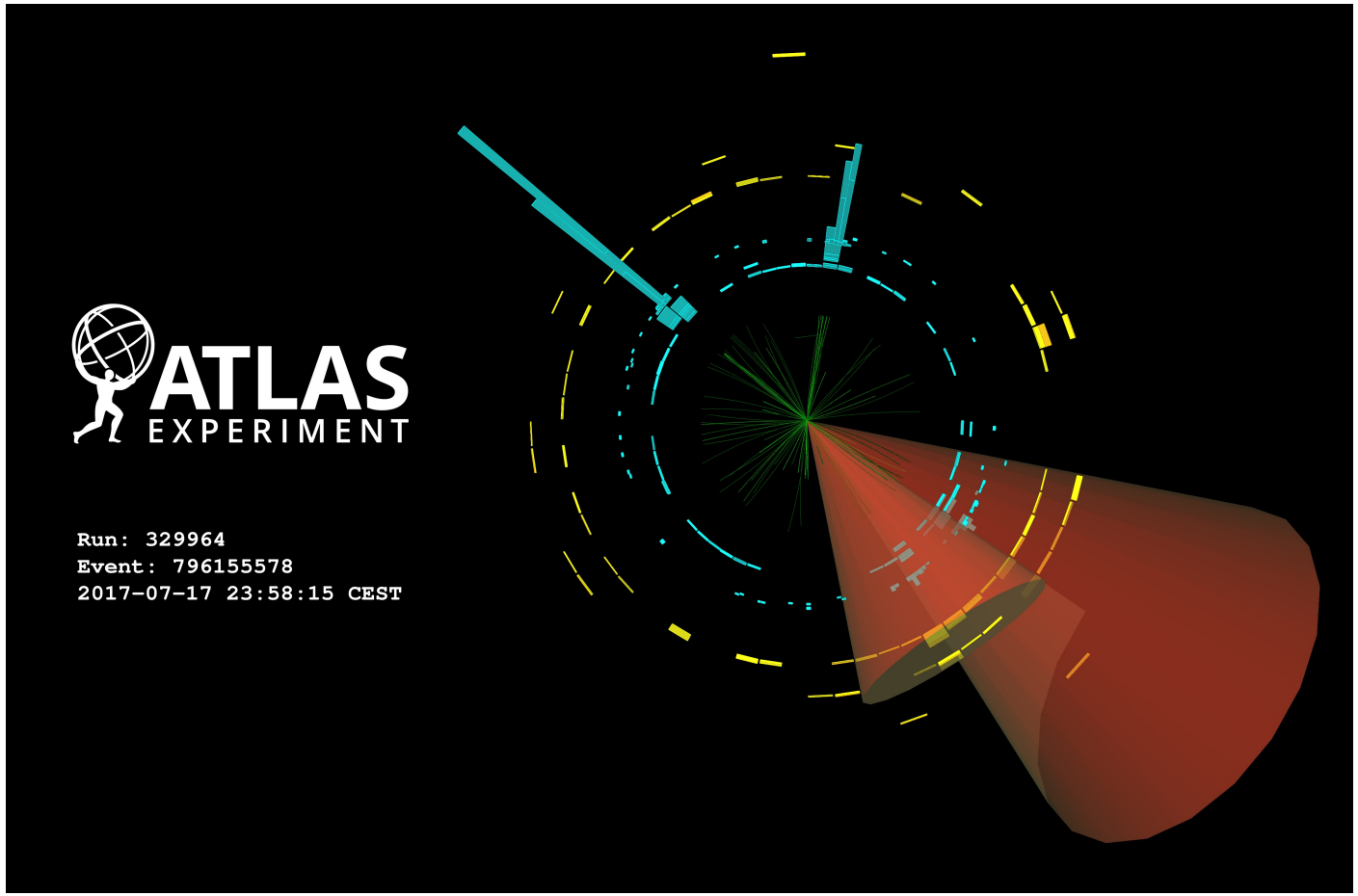

ATLAS-CONF-2021-016 (this talk)

JHEP 11 (2018) 040 (ATLAS 36 fb^{-1})

JHEP 03 (2021) 257 (CMS full Run2)

ATLAS-CONF-2021-052 (HH summary)

Motivation – HH production

Measuring **HH production** gives us access to the **trilinear Higgs self-coupling (λ_{HHH})**.

SM LHCHWGHH

Gluon-gluon fusion (ggFHH)

- σNNLO = **31.02** [fb] @13 TeV, mH = 125.09 GeV

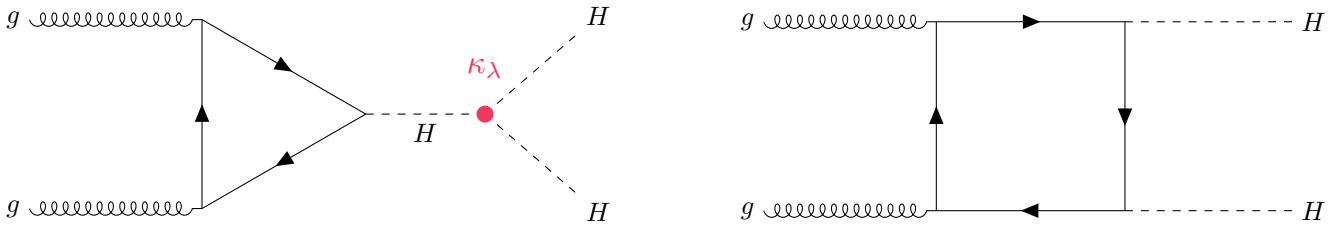

Vector boson fusion (VBFHH)

- σN3LO = **1.723** [fb] @13 TeV, mH = 125.09 GeV

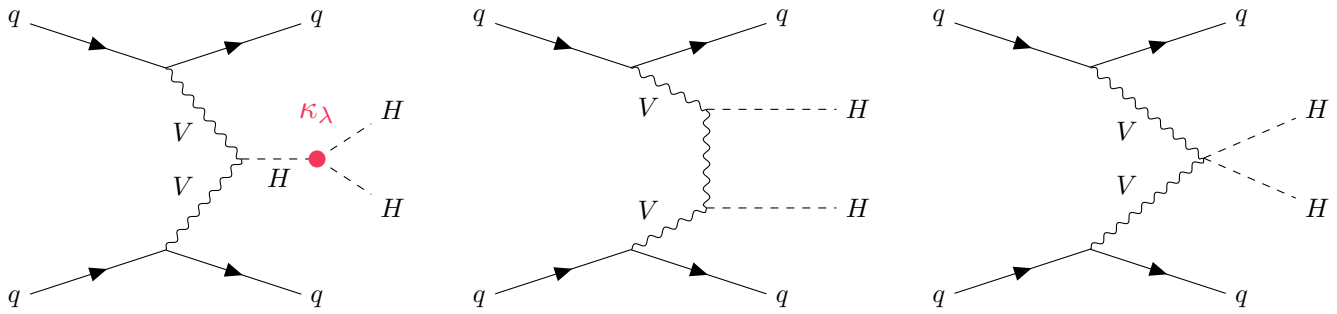

BSM enhancement

Non-resonant HH production

- Anomalous couplings ($\kappa_\lambda \neq 1$, etc.)

$$\kappa_\lambda = \frac{\lambda_{HHH}}{\lambda_{HHH}^{SM}}$$

Resonant HH production

Benchmark model:

X - a narrow-width scalar particle

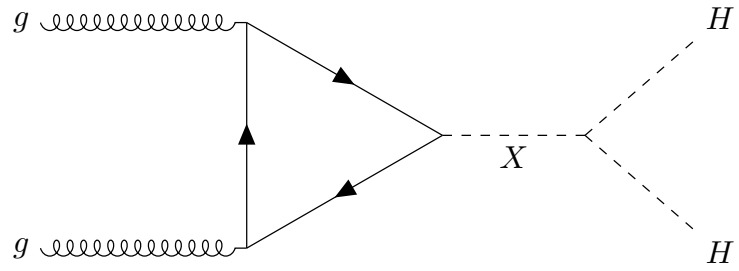

Motivation - $\gamma\gamma bb$ final state

$\gamma\gamma bb$ channel is one of the most sensitive HH final states.

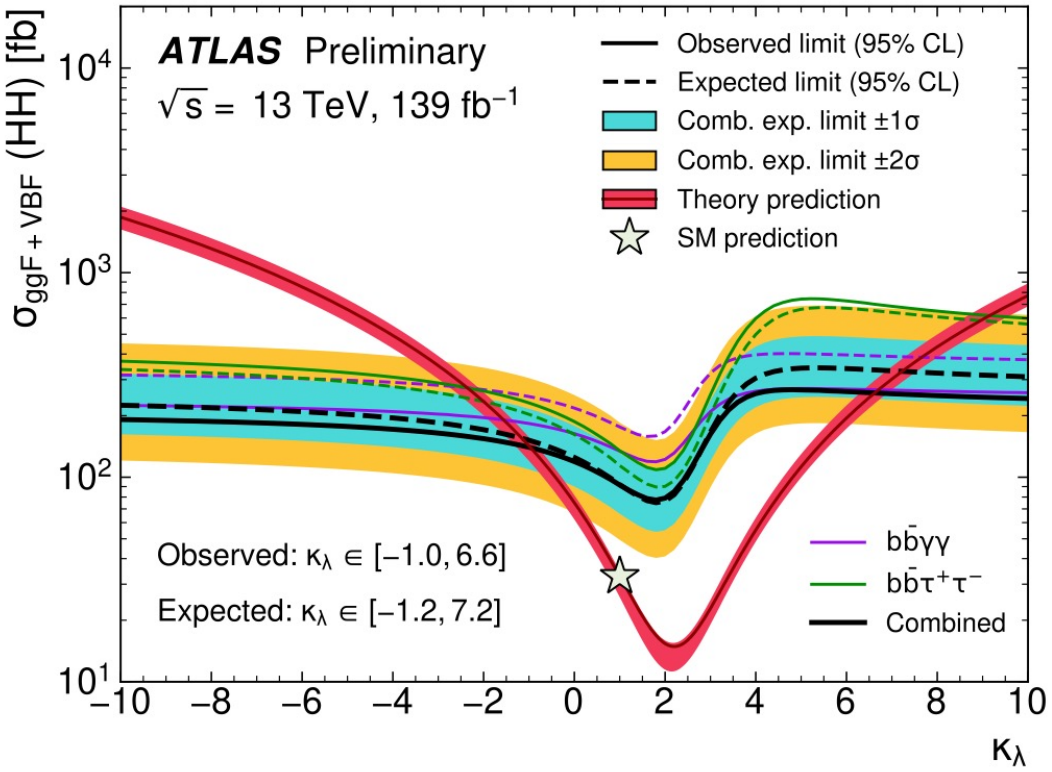

$\gamma\gamma$**bb**: advantage in κ_λ constraint

	bb	WW	ττ	ZZ	γγ
bb	34%				
WW	25%	4.6%			
ττ	7.3%	2.7%	0.39%		
ZZ	3.1%	1.1%	0.33%	0.069%	
γγ	0.26%	0.10%	0.028%	0.012%	0.0005%

$H \to bb$: Large **branching ratio**

$H \to \gamma\gamma$:

Excellent photon **resolution**

Relatively **small background**

Excellent handle for **trigger** (advantage for low m_{HH})

HH$\gamma\gamma bb$ Analysis overview

Search for **Non-resonant** and **Resonant** HH production in $\boldsymbol{\gamma\gamma bb}$ **channel** (full Run2 data, 139 fb^{-1}).

Main backgrounds

- Non-resonant $\gamma\gamma$ backgrounds
- Single Higgs production

Common Preselection

- Diphoton trigger
- Tight ID, calorimeter & track Isolation
- $p_T^{\gamma}/m_{\gamma\gamma}$> 0.25(0.35) for $\gamma_1(\gamma_2)$
- 105 GeV < $m_{\gamma\gamma}$ < 160 GeV
- Fewer than 6 central jets (reject hadronic top decays)
- Exactly 2 b-tagged jets (77% DL1r b-tagging efficiency)
- Veto events containing an electron or muon (reject leptonic top decays)

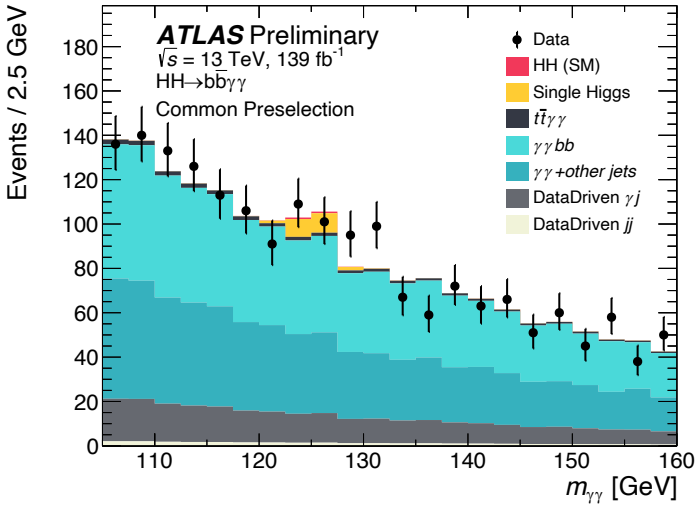

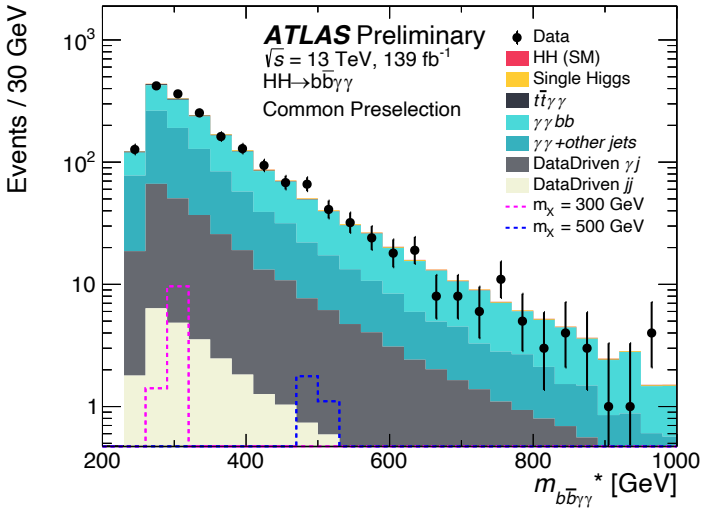

Categorization

For both Non-resonant and Resonant searches:

Signal regions are defined **using $m^*_{\gamma\gamma bb}$ and BDT score**

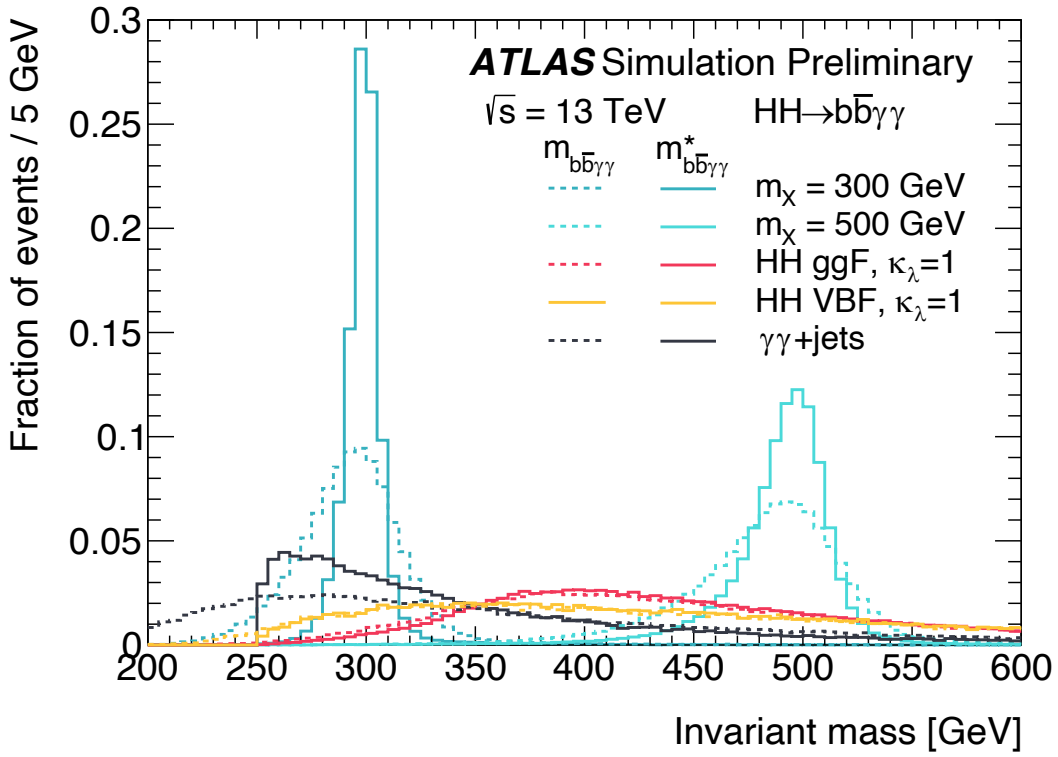

Modified invariant mass

$$m^*_{\gamma\gamma bb} = m_{\gamma\gamma bb} - m_{\gamma\gamma} - m_{bb} + 250\ GeV$$

- Provides cancellation of experimental resolution effects
  - Greater improvement for resonant signals

Non-resonant Categorization

Non-resonant analysis: target SM HH → $\gamma\gamma bb$ processes, and possible modifications to κ_λ.

Target mainly ggF HH production, but VBF HH events also considered as signal.

- **Modified invariant mass** $m^*_{\gamma\gamma bb} = m_{\gamma\gamma bb} - m_{\gamma\gamma} - m_{bb} + 250\ GeV$
- **Low** and **high** mass categories provide enhanced sensitivity to κ_λ

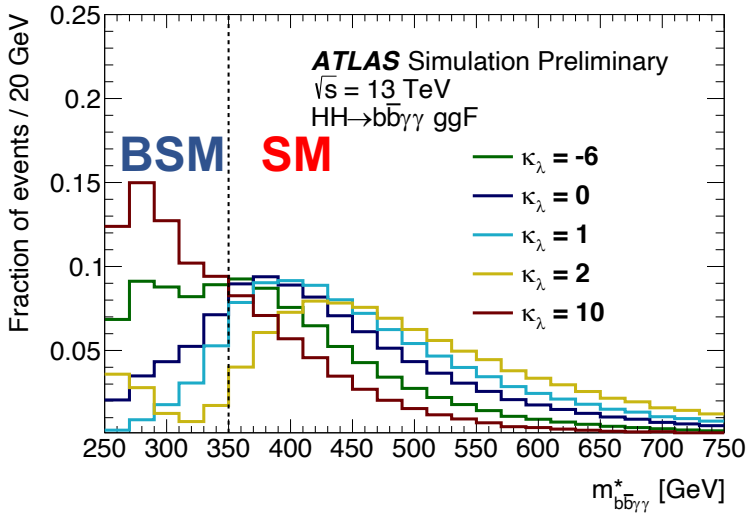

Low mass region
Targeting BSM
$m^*_{\gamma\gamma bb} < 350\ GeV$

High mass region
Targeting SM
$m^*_{\gamma\gamma bb} > 350\ GeV$

Non-resonant Categorization

Non-resonant analysis: target SM HH → $\gamma\gamma bb$ processes, and possible modifications to κ_λ.

Target mainly ggF HH production, but VBF HH events also considered as signal.

- **Modified invariant mass $m^*_{\gamma\gamma bb} = m_{\gamma\gamma bb} - m_{\gamma\gamma} - m_{bb} + 250\ GeV$**
- **Low** and **high** mass categories provide enhanced sensitivity to κ_λ
- **Boosted Decision Tree**
- Against $\gamma\gamma$ and single Higgs backgrounds
- BDT trained on photon, jet and missing transverse energy variables

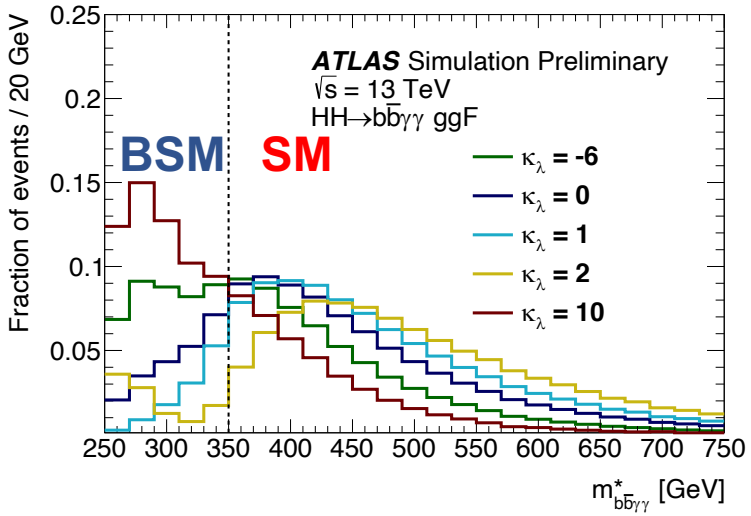

Low mass region
Targeting BSM
$m^*_{\gamma\gamma bb} < 350\ GeV$
- BDT Loose
- BDT Tight

High mass region
Targeting SM
$m^*_{\gamma\gamma bb} > 350\ GeV$
- BDT Loose
- BDT Tight

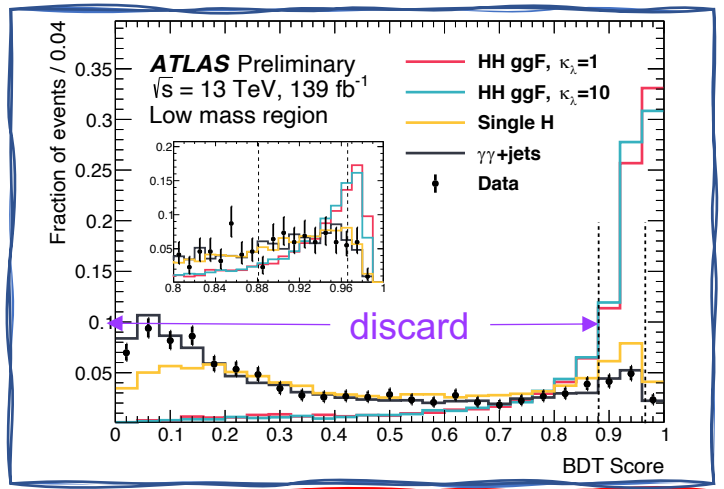

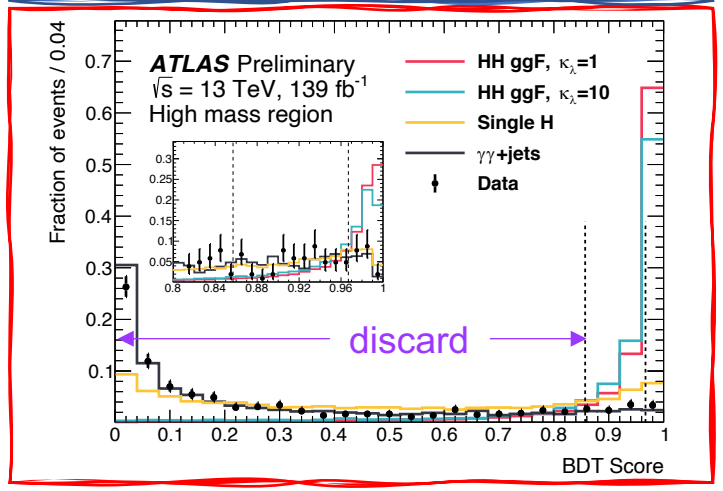

Resonant Categorization

Resonant analysis: target BSM HH $\rightarrow X \rightarrow \gamma\gamma bb$ processes, with $m_X \in [251, 1000]$ GeV.

Non-resonant SM HH production included as background.

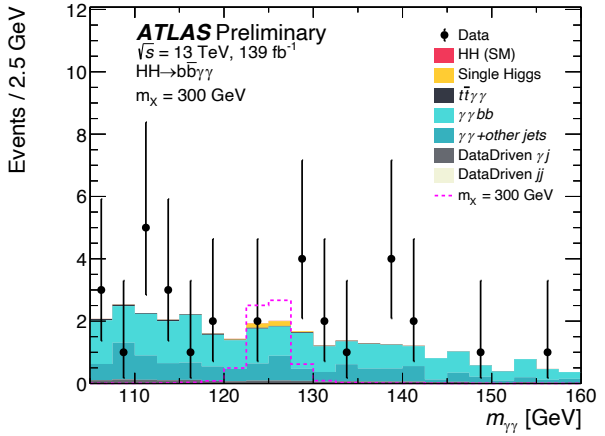

➢ **Modified invariant mass** $m^*_{\gamma\gamma bb} = m_{\gamma\gamma bb} - m_{\gamma\gamma} - m_{bb} + 250\ GeV$

- $\pm 2\sigma$ window cut around each mass hypothesis of the resonance
  - $\pm 4\sigma$ cut for m_X = 900, 1000 GeV due to the lack of background statistics

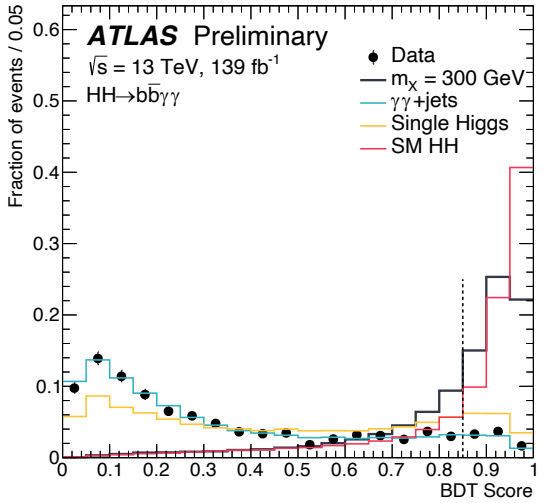

➢ **Boosted Decision Tree**

- Shared by all resonance masses to avoid lack of background at high mass
- BDTs trained on photon, jet and missing transverse energy variables
- 2 BDTs against $\gamma\gamma$+$tt\gamma\gamma$ and single Higgs backgrounds respectively
- For each m_X, cut on the **combined BDT score**

Signal and background modeling

Maximum likelihood fit performed on $m_{\gamma\gamma}$ simultaneously with all the categories.
(Non-resonant: 4 categories; Resonant: 1 category for each m_X)

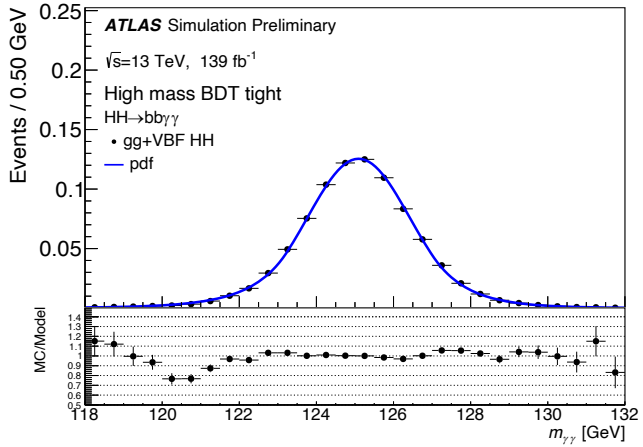

➢ Signal parameterization

Normalization fixed to SM, shape from a **double sided crystal ball (DSCB)** fit to MC

Non-resonant

- Fit to SM $\boldsymbol{HH}$ signal, model shared with $\boldsymbol{H}$ background

Resonant

- Fit to resonance signals, model shared with SM $\boldsymbol{HH}$ and $\boldsymbol{H}$ background

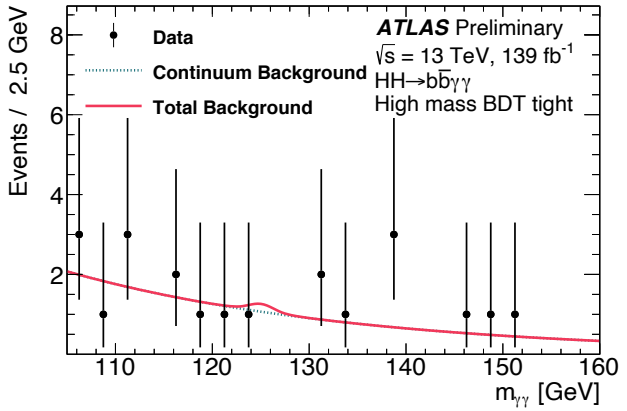

➢ Background parameterization

Normalization floating, shape = **exponential function**

- Function form determined from **spurious signal** studies.
- **Spurious signal** (potential bias due to choice of function) estimated by fitting S+B to B-only template.

Observed (Expected) Results

No signal is observed, **upper Limits at 95%CL** are set based on the profile likelihood ratio approach.

Non-resonant

- μ_{HH} **limit**: 4.1 x SM (5.5 x SM)
- κ_λ **interval**: [−1.5, 6.7] ([−2.4, 7.7])

~ 5 improvement w.r.t 36 fb^{-1}
~2 from increase of lumi
~2.5 from analysis strategy

Shrinks by a factor of ~2

ATLAS 36 fb^{-1} JHEP 11 (2018) 040
μ_{HH} **limit:** 22 (28) x SM
κ_λ **interval:** [-8.2, 13.2] ([-8.3, 13.2])

CMS full Run2 JHEP 03 (2021) 257
μ_{HH} **limit:** 7.7 (5.2) x SM
κ_λ **interval:** [-3.3, 8.5] ([-2.5, 8.2])

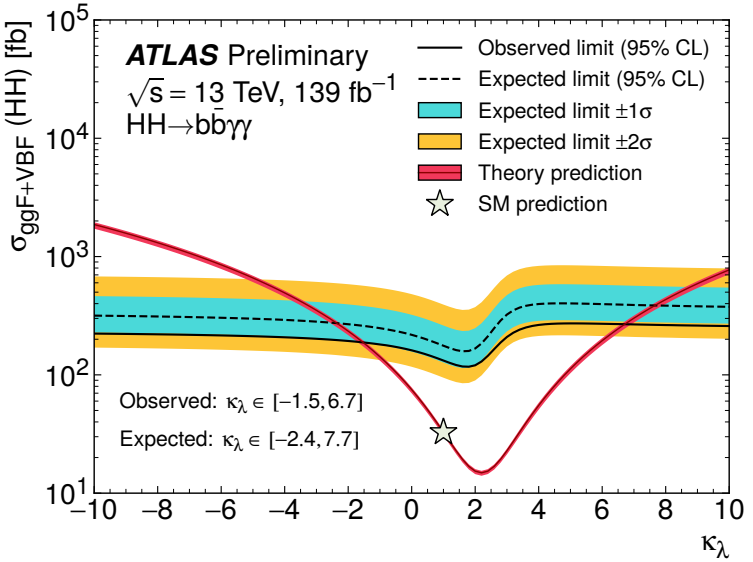

Resonant

- **XS upper limits** vary between 610-47 fb (360-43 fb) in $251 \leq m_X \leq 1000$ GeV

~2-3 improvement depending on the m_X value

~2 from increase of lumi; ~1.2 from analysis strategy

Expands the analyzed mass range of the resonance search to lower values.

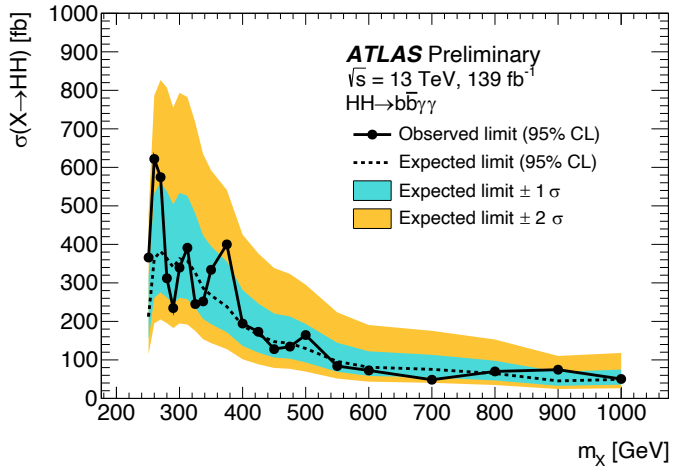

Summary

Searches for non-resonant and resonant HH production are performed in the $bb\gamma\gamma$ final state (139 fb^{-1}).

No significant excess with respect to the SM background expectation is observed.

Both **limited by statistics**. Dominant systematic: spurious signal.

Improvement compared to the previous ATLAS result based on 36 fb^{-1} of 13 TeV pp collisions

- Extends the data set by more than a factor of 4
- Incorporates a categorization based on $m^{*}_{\gamma\gamma bb}$ and multivariate event selections
- More precise object reconstruction and calibration

Publication of the Run 2 paper soon.

Preparing the dedicated analysis for VBFHH and SH → $bb\gamma\gamma$ signals.

中国科学院高能物理研究所
Institute of High Energy Physics
Chinese Academy of Sciences

NANJING UNIVERSITY 1902

ATLAS EXPERIMENT

Thanks!

Motivation – Higgs self-coupling

- **The Higgs boson** completes the Standard Model of Particle Physics.
- However, the shape of **the Higgs potential** has yet to be measured.
- We can probe the Higgs potential by measuring the **Higgs self-coupling (λ).**

$$V(\phi) = -\mu^2\phi^2 + \lambda\phi^4$$

$$V(\nu + h) = V_0 + \frac{1}{2}{m_h}^2h^2 + \lambda v h^3 + \lambda h^4 + \ldots$$

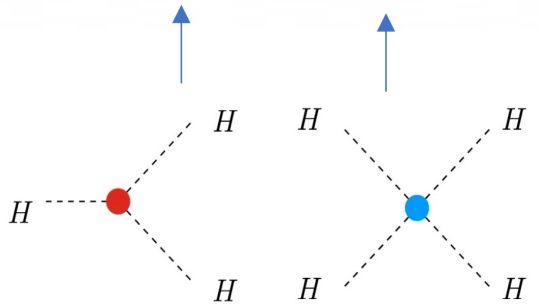

$$\kappa_\lambda = \frac{\lambda_{HHH}}{\lambda_{HHH}^{SM}}$$

Resonant Higgs Pair Production

LHC seminar Nov-23

New physics is *required* if $\kappa_\lambda \neq 1$

Many beyond the Standard Model theories predict new particles that can decay to a pair of Higgs bosons

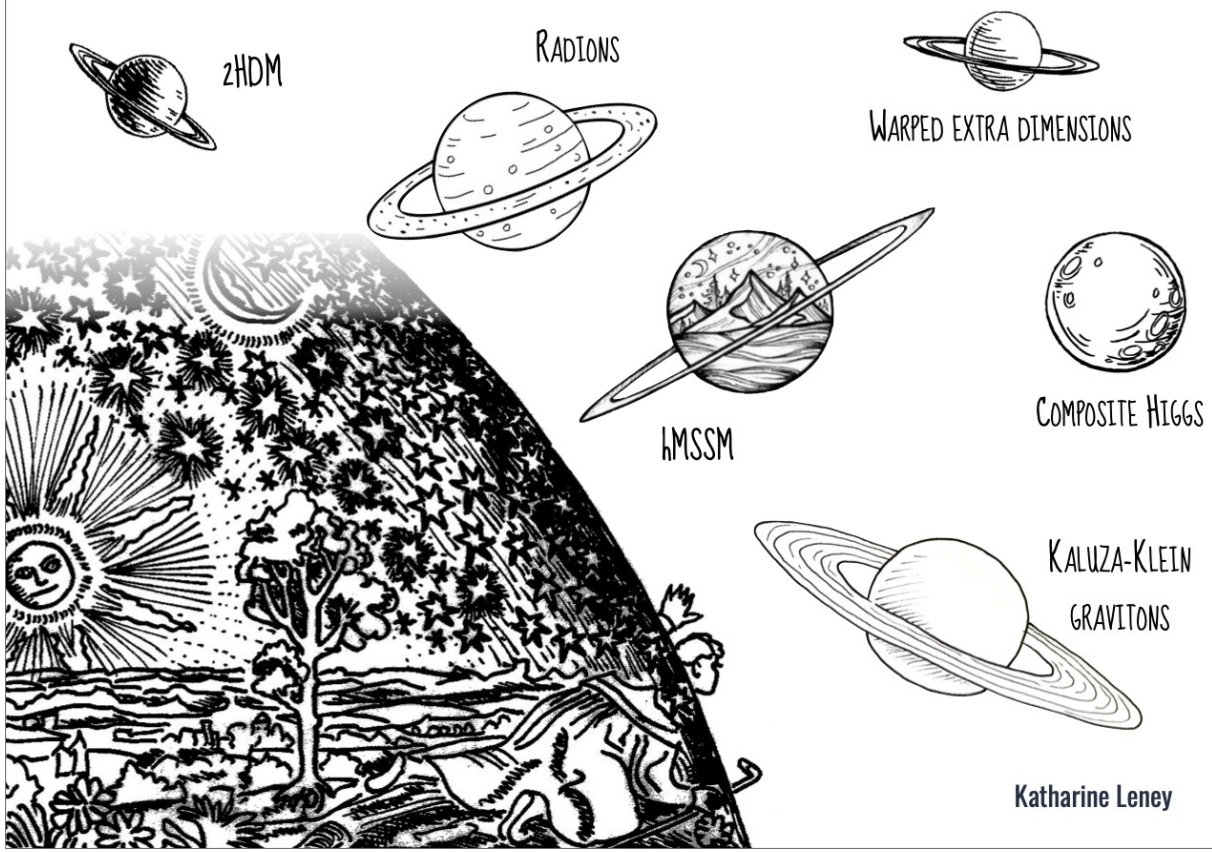

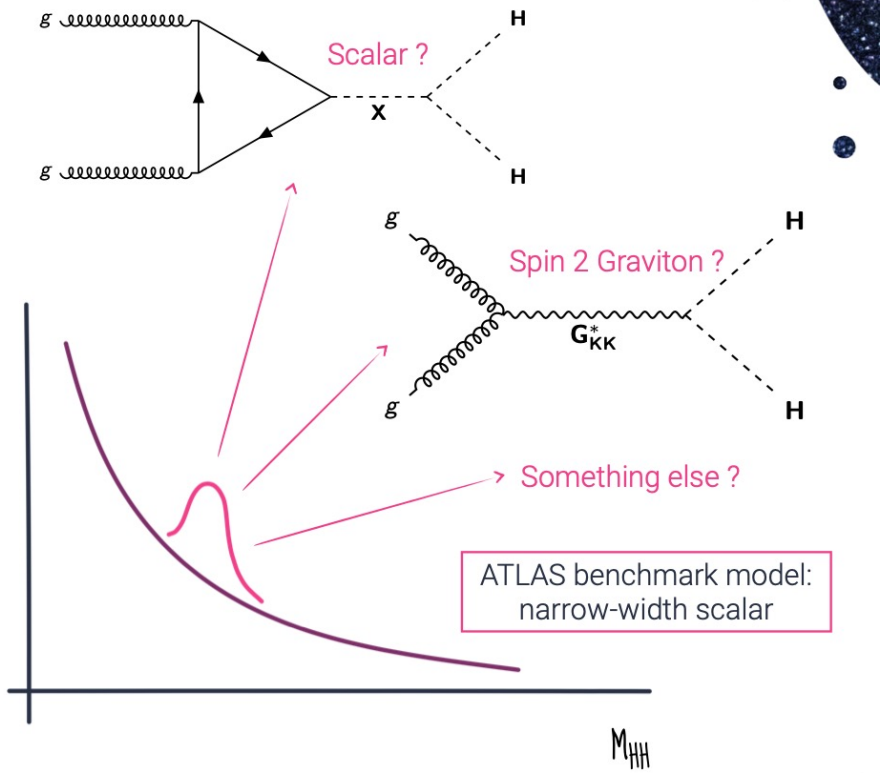

14

Overview

$HH \to b\bar{b}\gamma\gamma$ analysis in a nutshell

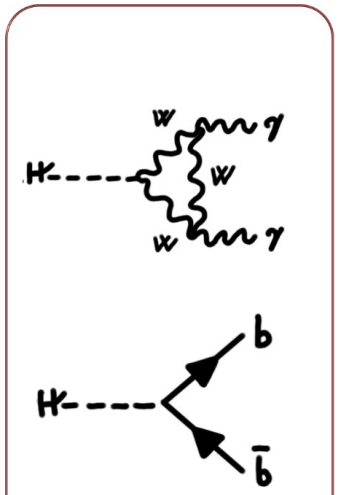

Object selection

Event categorization

MVA approach

4 categories for non-resonant analysis

1 category per m_X for resonant analysis

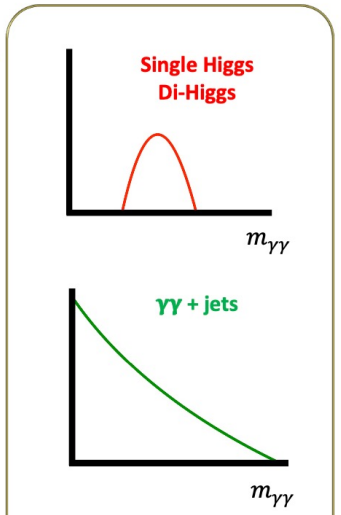

Modelling of discriminant variable

Simultaneous likelihood fit to all categories

SM σ limits and **σ vs k_λ** for non resonant analysis

σ vs m_X for resonant analysis

Statistically limited with the current dataset

Background Samples

Table 1: Summary of single Higgs boson background samples, split by production modes, and continuum background samples. The generator used in the simulation, the PDF set, and tuned parameters (tune) are also provided.

Process	Generator	PDF set	Showering	Tune
ggF	NNLOPS [65–67] [68, 69]	PDFLHC [42]	Pythia 8.2 [70]	AZNLO [71]
VBF	Powheg Box v2 [39, 66, 72–78]	PDFLHC	Pythia 8.2	AZNLO
WH	Powheg Box v2	PDFLHC	Pythia 8.2	AZNLO
$qq \to ZH$	Powheg Box v2	PDFLHC	Pythia 8.2	AZNLO
$gg \to ZH$	Powheg Box v2	PDFLHC	Pythia 8.2	AZNLO
$t\bar{t}H$	Powheg Box v2 [73–75, 78, 79]	`NNPDF3.0nlo` [80]	Pythia 8.2	A14 [81]
bbH	Powheg Box v2	`NNPDF3.0nlo`	Pythia 8.2	A14
$tHqj$	MadGraph5_aMC@NLO	`NNPDF3.0nlo`	Pythia 8.2	A14
tHW	MadGraph5_aMC@NLO	`NNPDF3.0nlo`	Pythia 8.2	A14
$\gamma\gamma$+jets	Sherpa v2.2.4 [56]	`NNPDF3.0nnlo`	Sherpa v2.2.4	–
$t\bar{t}\gamma\gamma$	MadGraph5_aMC@NLO	`NNPDF2.3lo`	Pythia 8.2	–

Common selections

Di-photon triggers with E_T **> 35, 25 GeV**. Trigger efficiency for the non-resonant signal is 82.9% and 69.5% for the resonant signal (using as reference m_X = 300 GeV).

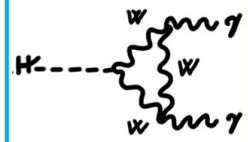

At least **2 photons**:

- Identified (Tight WP)
- Calo- and Track-isolated within a cone of $\Delta R = 0.2$
  - $E_T^{iso} < 0.065 \cdot E_T$ and $p_T^{iso} < 0.05 \cdot E_T$
- 105 GeV < $m\gamma\gamma$ < 160 GeV
- $E_T/m\gamma\gamma$ > 0.35 and 0.25
- γγ vertex

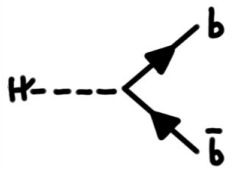

Less than 6 central jets (reduce ttH)

- PFlow jets, anti-kt R=0.4, tight JVT applied

Exactly **2 b-jets**

- DL1r 77% WP
- B-jet energy corrections applied →
  - Muon-in-jet
  - pT-reco

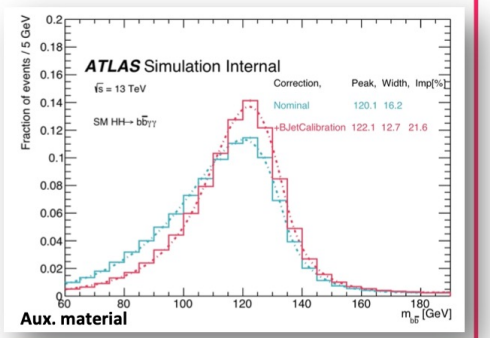

Lepton veto: Events are rejected if they contain medium electrons and/or medium muons

H(bb)

1. PFlow jets (AntiKt4PFlowCustomVtxHggJets) with pT > 25 GeV and $|\eta|$<2.5 passing JetVertexFraction (JVT) tight and Jet cleaning
2. Exactly 2 b-jets passing the 77% DL1r b-tagging WP and ranked by pT

- **mbb resolution** improved by a muon-in-jet correction, as well as a pT-reco correction to account for pT loss due to neutrinos and objects outside of the jet cone. **Resolution improves by about 22%**

Flavour-Tagging Improvements

FTAG-2019-005

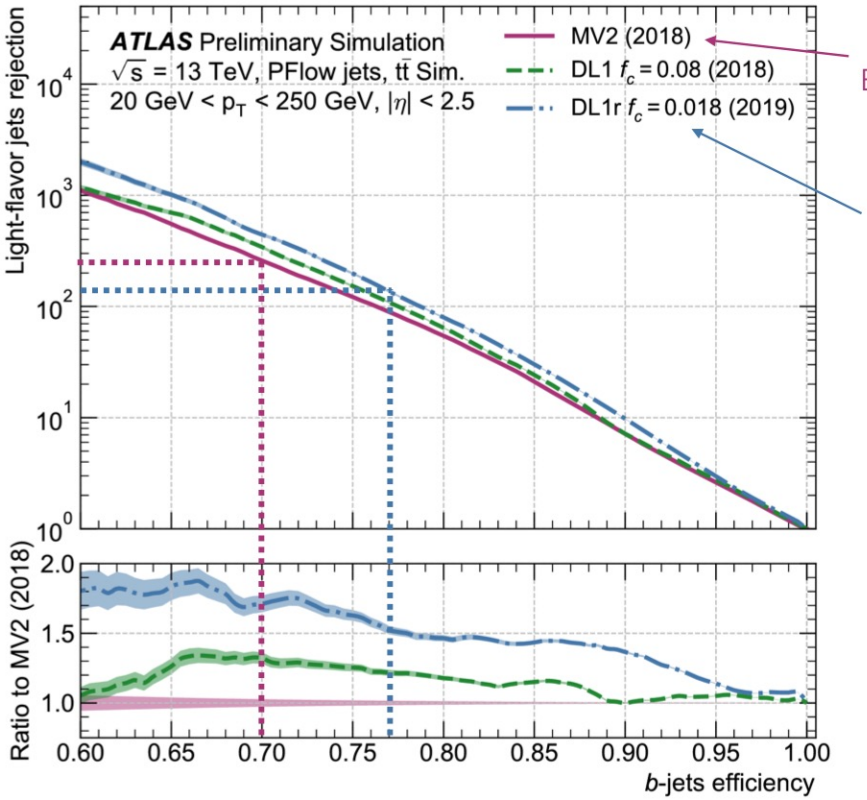

MV2 (USED FOR 2015+2016 RESULTS)
BDT combining outputs of low-level taggers - IP3D, SV1 and JetFitter

DL1R (NEW)
Deep feed-forward neural network using same inputs and multi-dimensional outputs - P(light), P(c-jet), P(b-jet)

All HH analyses able to move to a higher efficiency working point.

Per-b-jet tagging efficiency increased 70% → 77%

(x 2 or 4 b-jets per event)

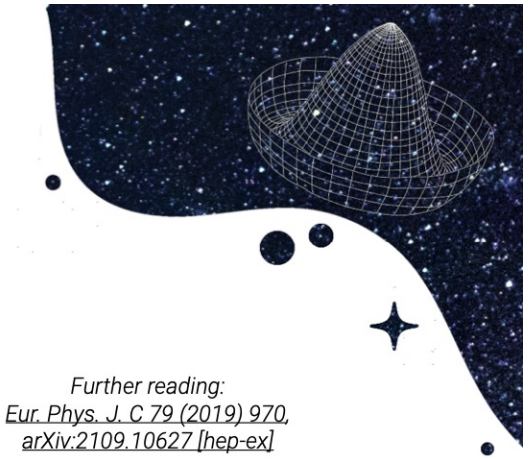

Further reading:
Eur. Phys. J. C 79 (2019) 970, arXiv:2109.10627 [hep-ex]

FTAG-2021-001

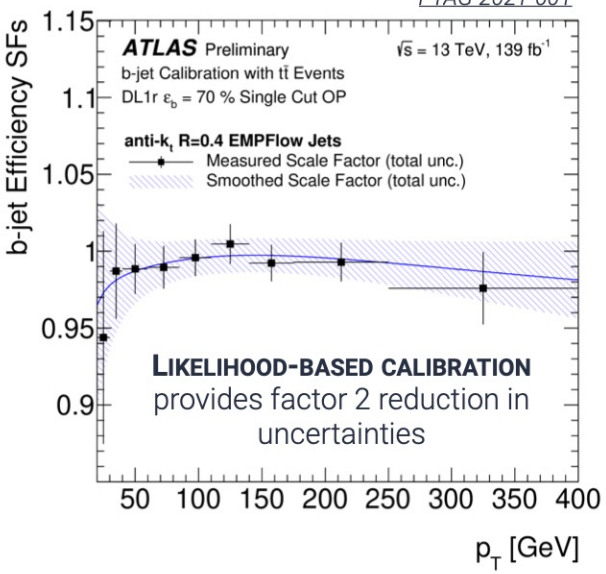

LIKELIHOOD-BASED CALIBRATION provides factor 2 reduction in uncertainties

Non-resonant BDT variables

Table 2: Variables used in the BDT for the non-resonant analysis. The b-tag status identifies the highest fixed b-tag working point (60%, 70%, 77%) that the jet passes. All vectors in the event are rotated so that the leading photon ϕ is equal to zero.

Variable	Definition
Photon-related kinematic variables	
$p_{\mathrm{T}}/m_{\gamma\gamma}$	Transverse momentum of the two photons scaled by their invariant mass $m_{\gamma\gamma}$
η and ϕ	Pseudo-rapidity and azimuthal angle of the leading and sub-leading photon
Jet-related kinematic variables	
b-tag status	Highest fixed b-tag working point that the jet passes
p_{T}, η and ϕ	Transverse momentum, pseudo-rapidity and azimuthal angle of the two jets with the highest b-tagging score
$p_{\mathrm{T}}^{b\bar{b}}$, $\eta_{b\bar{b}}$ and $\phi_{b\bar{b}}$	Transverse momentum, pseudo-rapidity and azimuthal angle of b-tagged jets system
$m_{b\bar{b}}$	Invariant mass built with the two jets with the highest b-tagging score
H_{T}	Scalar sum of the p_{T} of the jets in the event
Single topness	For the definition, see Eq. (1)
Missing transverse momentum-related variables	
$E_{\mathrm{T}}^{\mathrm{miss}}$ and ϕ^{miss}	Missing transverse momentum and its azimuthal angle

highest discriminating power: m_{bb} and H_T

$$\chi_{Wt} = \min \sqrt{\left(\frac{m_{j_1 j_2} - m_W}{m_W}\right)^2 + \left(\frac{m_{j_1 j_2 j_3} - m_t}{m_t}\right)^2},$$

Non-resonant Categorization

$$Z = \sqrt{2 * [(s+b) * \log(1+s/b) - s]}$$

Low mass region

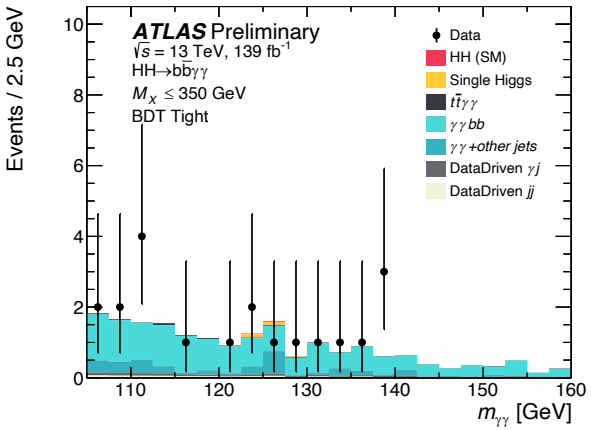

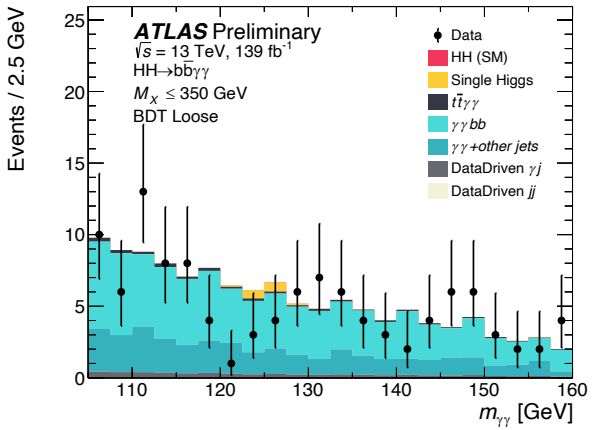

High mass region

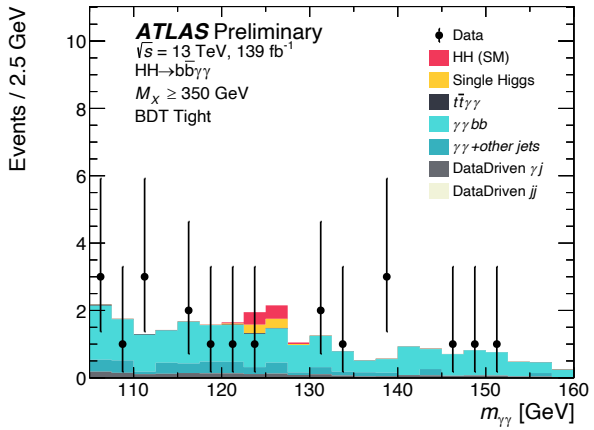

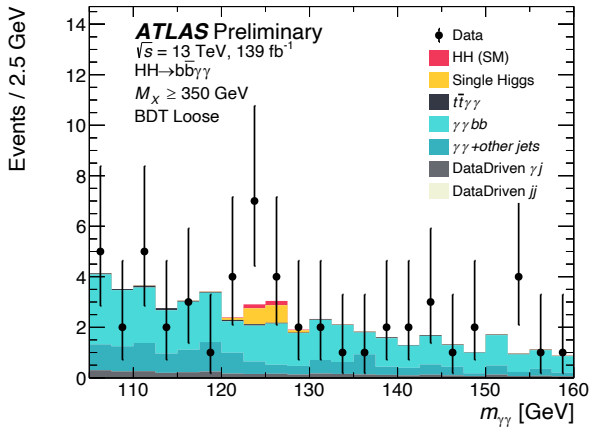

Resonant BDT variables

Table 4: Variables used in the BDT for the resonant analysis. For variables depending on b-tagged jets, only jets b-tagged using the 77% working point are considered as described in Section 4.1.

Variable	Definition
Photon-related kinematic variables	
$p_{\mathrm{T}}^{\gamma\gamma}$, $y^{\gamma\gamma}$	Transverse momentum and rapidity of the di-photon system
$\Delta\phi_{\gamma\gamma}$ and $\Delta R_{\gamma\gamma}$	Azimuthal angular distance and ΔR between the two photons
Jet-related kinematic variables	
$m_{b\bar{b}}$, $p_{\mathrm{T}}^{b\bar{b}}$ and $y_{b\bar{b}}$	Invariant mass, transverse momentum and rapidity of the b-tagged jets system
$\Delta\phi_{b\bar{b}}$ and $\Delta R_{b\bar{b}}$	Azimuthal angular distance and ΔR between the two b-tagged jets
N_{jets} and $N_{b-\mathrm{jets}}$	Number of jets and number of b-tagged jets
H_{T}	Scalar sum of the p_{T} of the jets in the event
Photons and jets-related kinematic variables	
$m_{b\bar{b}\gamma\gamma}$	Invariant mass built with the di-photon and b-tagged jets system
$\Delta y_{\gamma\gamma,b\bar{b}}$, $\Delta\phi_{\gamma\gamma,b\bar{b}}$ and $\Delta R_{\gamma\gamma,b\bar{b}}$	Distance in rapidity, azimuthal angle and ΔR between the di-photon and the b-tagged jets system

$$\mathrm{BDT}_{\mathrm{tot}} = \frac{1}{\sqrt{C_1^2 + C_2^2}} \sqrt{C_1^2 \left(\frac{\mathrm{BDT}_{\gamma\gamma} + 1}{2}\right)^2 + C_2^2 \left(\frac{\mathrm{BDT}_{\mathrm{Single}H} + 1}{2}\right)^2}$$

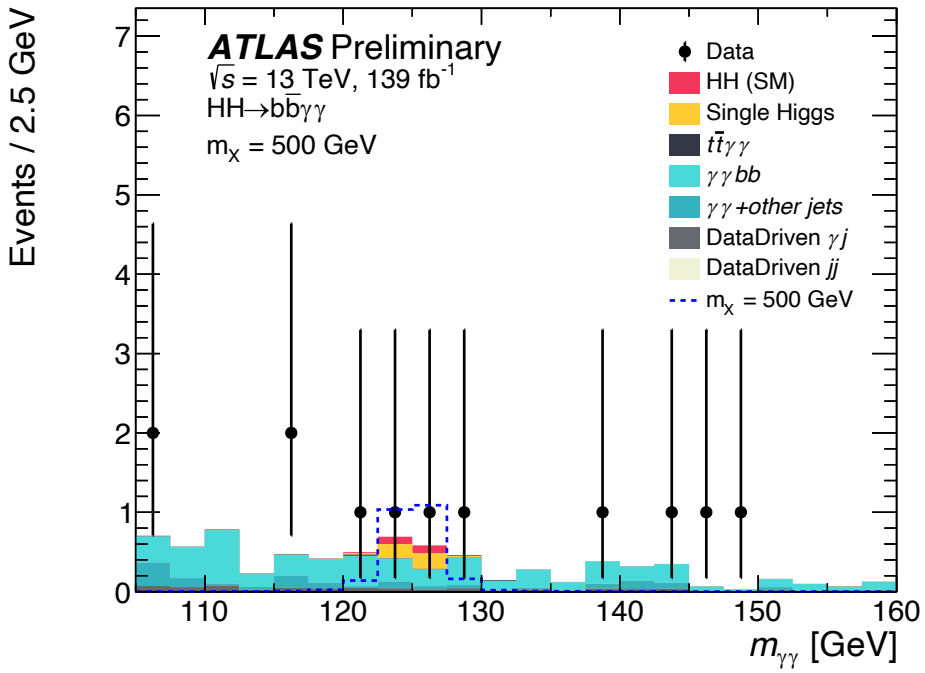
ATLAS Preliminary
√s = 13 TeV, 139 fb-1
HH→bb̄γγ
mX = 500 GeV
Data
HH (SM)
Single Higgs
tt̄γγ
γγbb
γγ+other jets
DataDriven γj
DataDriven jj
mX = 500 GeV
Events / 2.5 GeV
mγγ [GeV]

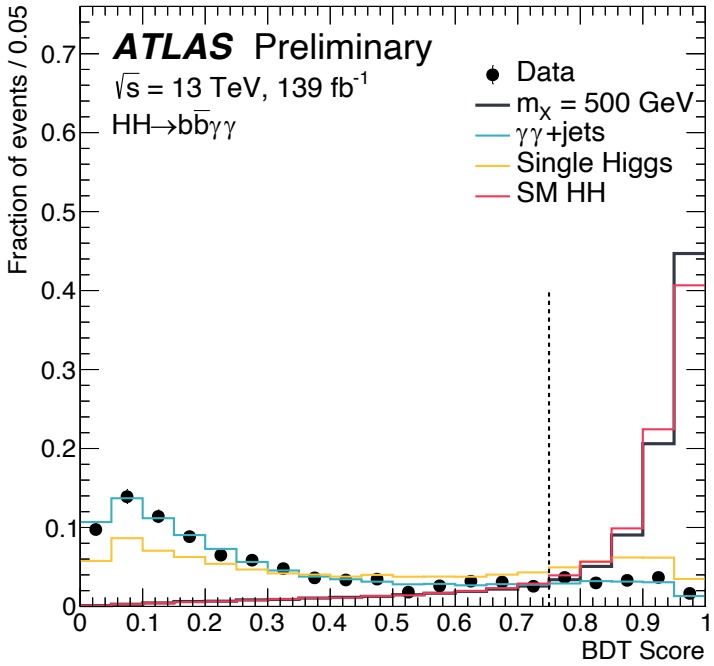
ATLAS Preliminary
√s = 13 TeV, 139 fb-1
HH→bb̄γγ
Data
mX = 500 GeV
γγ+jets
Single Higgs
SM HH
Fraction of events / 0.05
BDT Score

Signal modeling - DSCB

A Gaussian core + asymmetric power law tails

$$f_{\mathrm{DSCB}}(m_{\gamma\gamma}) = N \times \begin{cases} e^{-t^2/2} & \text{if } -\alpha_{low} \le t \le \alpha_{high} \\ \dfrac{e^{-\frac{1}{2}\alpha_{low}^2}}{\left[\frac{1}{R_{low}}\left(R_{low} - \alpha_{low} - t\right)\right]^{n_{low}}} & \text{if } t < -\alpha_{low} \\ \dfrac{e^{-\frac{1}{2}\alpha_{high}^2}}{\left[\frac{1}{R_{high}}\left(R_{high} - \alpha_{high} + t\right)\right]^{n_{high}}} & \text{if } t > \alpha_{high} \end{cases}$$

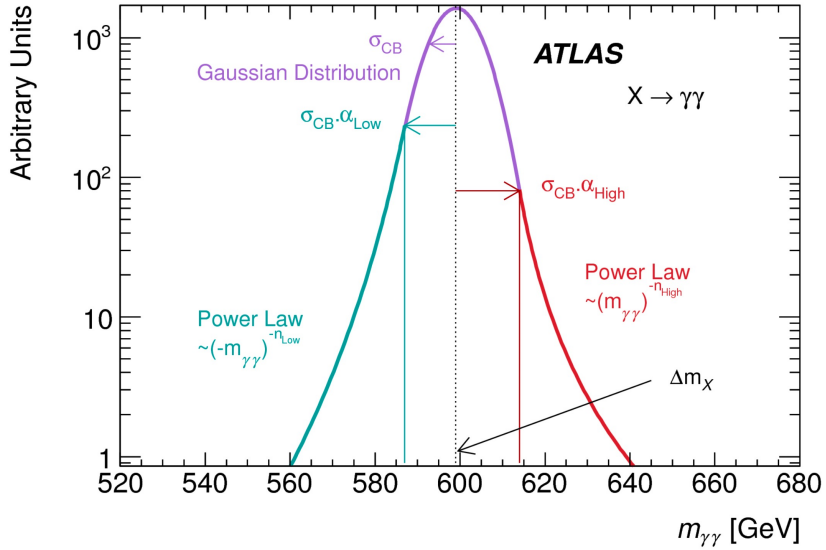

where N is a normalization factor and the six parameters are

- μ_{CB} and σ_{CB} describe the mean and the width of the Gaussian core, which are combined in $t = \left(m_{\gamma\gamma} - \mu_{\mathrm{CB}}\right)/\sigma_{\mathrm{CB}}$;
- α_{low} and α_{high} are the positions of the transitions with respect to μ_{CB} from the Gaussian core to power-law tails, in unit of σ_{CB}, on the low and high mass sides respectively;
- n_{low} and n_{high} are the exponents of the low and high mass tails. With the α's, they define $R_{low} = \frac{n_{low}}{\alpha_{low}}$ and R_{high} similarly.

Diphoton background decomposition

Reconstructed $\gamma\gamma$ events is mainly composed of $\gamma\gamma$, γ-jets and jet-jet events, where the jet(s) fake(s) a real photon. **The 2x2D sideband method** is developed using the discriminating power of photon identification and isolation criteria. **The event yields** in the signal region and the 15 sidebands can be expressed as **functions** of the photon efficiencies, jet fake rates and correlation coefficients.

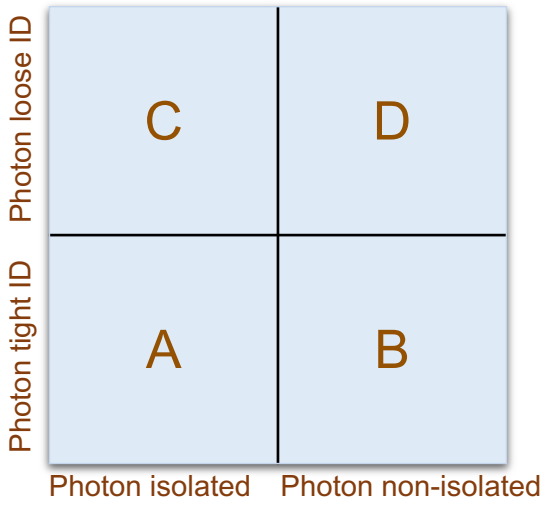

Leading object

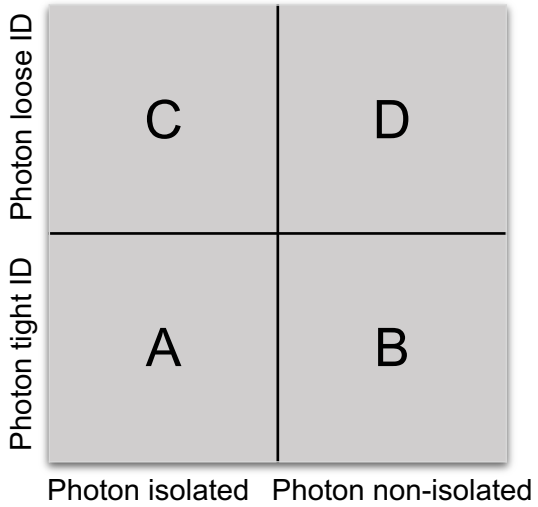

Sub-leading object

CC	CD	DC	DD
CA	CB	DA	DB
AC	AD	BC	BD
AA	AB	BA	BB

Suffers from low statistics, not used in constructing the background templates for the spurious signal procedure.

Spurious signal

Spurious signal: bias estimated from a signal + background fit to a background-only MC template.

$$N_{sp} = \max_{121<m_H<129\,GeV} |N_s(m_H)|$$

➢ **Selection criteria:**

☐ The function should satisfy at least one of the following criteria:

Nominal criteria

$N_{sp} < 10\%\ N_{s,exp}$

or

$N_{sp} < 20\%\ \sigma_{bkg}$

Relaxed criteria (for low-statistic bkg MC)

$$\boldsymbol{N_{sp}} = \zeta_s(m_{\gamma\gamma}) = \begin{cases} N_s + 2\Delta_{MC}, & N_s + 2\Delta_{MC} < 0 \\ N_s - 2\Delta_{MC}, & N_s - 2\Delta_{MC} > 0 \\ 0, & \text{otherwise} \end{cases}$$

- $N_{s,exp}$ = expected SM signal events
- σ_{bkg} = stat. uncertainty on Nsig when fitting the sig+bkg model to the asimov dataset
- Δ_{MC} = local statistical fluctuation of the MC background template

☐ The function must satisfy a simple χ^2 requirement in a background-only fit to the MC template:

$$p - value(\chi^2) > 1\%$$

The χ^2 is computed with a background template uniformly binned over 105 < $m\gamma\gamma$ < 160 GeV.

➢ **The least number of parameters** is preferred.

➢ The **smaller systematic uncertainty** (spurious signal) is preferred.

Bkg templates from MC

Wald test

Wald test: un-bin fit on data sideband to reject simpler background function for **low statistic categories.**

We restrict the function options to **exponential of 1st, 2nd and 3rd order**:

$$f_i x = e^{\Sigma_{i=0}^{2} a_i x^i}, \quad x = \mathrm{m}_{\gamma\gamma}$$

Define the test statistics using the likelihood values of the two fits L_1 and L_2:

$$\lambda_{1,2} = -2 \ln \left(\frac{L_1}{L_2} \right)$$

Check the P-value $P(\lambda \geq \lambda_{data})$. Only if the **P-value < 0.05** will we reject the simpler function.

Wald tests show that the data do not prefer a higher degree functional form with respect to the exponential form.

Systematic uncertainties

In general the analysis is almost completely statistically dominated with the Run 2 dataset

		Relative impact of the systematic uncertainties in %	
Source	Type	Non-resonant analysis HH	Resonant analysis m_X = 300 GeV
Experimental			
Photon energy scale	Norm. + Shape	5.2	2.7
Photon energy resolution	Norm. + Shape	1.8	1.6
Flavor tagging	Normalization	0.5	< 0.5
Theoretical			
Heavy flavor content	Normalization	1.5	< 0.5
Higgs boson mass	Norm. + Shape	1.8	< 0.5
PDF+α_s	Normalization	0.7	< 0.5
Spurious signal	Normalization	5.5	5.4

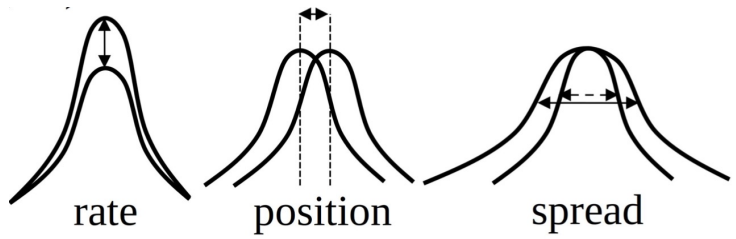

Statistical model

Likelihood

$$\mathcal{L} = \prod_c \left(\text{Pois}(n_c | N_c(\boldsymbol{\theta})) \cdot \prod_{i=1}^{n_c} f_c(m^i_{\gamma\gamma}, \boldsymbol{\theta}) \cdot G(\boldsymbol{\theta}) \right)$$

Expected number of events

$$N_c(\boldsymbol{\theta}) = \mu \cdot N_{HH,\mathrm{c}}(\boldsymbol{\theta}^{\mathrm{yield}}_{HH}) + N^{\mathrm{res}}_{\mathrm{bkg,c}}(\boldsymbol{\theta}^{\mathrm{yield}}_{\mathrm{res}}) + N_{\mathrm{SS,c}} \cdot \boldsymbol{\theta}^{\mathrm{SS,c}} + N^{\mathrm{non-res}}_{\mathrm{bkg,c}}$$

Model PDF

$$f_c(m_{\gamma\gamma}, \boldsymbol{\theta}) = [\mu \cdot N_{HH,\mathrm{c}}(\boldsymbol{\theta}^{\mathrm{yield}}_{HH}) \cdot f_{HH,\mathrm{c}}(m_{\gamma\gamma}, \boldsymbol{\theta}^{\mathrm{shape}}_{HH}) + N^{\mathrm{res}}_{\mathrm{bkg,c}}(\boldsymbol{\theta}^{\mathrm{yield}}_{\mathrm{res}}) \cdot f^{\mathrm{res}}_{\mathrm{bkg,c}}(m_{\gamma\gamma}, \boldsymbol{\theta}^{\mathrm{shape}}_{\mathrm{res}})$$
$$+ N_{\mathrm{SS,c}} \cdot \boldsymbol{\theta}^{\mathrm{SS,c}}_{HH} \cdot f_{HH,\mathrm{c}}(m_{\gamma\gamma}, \boldsymbol{\theta}^{\mathrm{shape}}_{HH}) + N^{\mathrm{non-res}}_{\mathrm{bkg,c}} \cdot f^{\mathrm{non-res}}_{\mathrm{bkg,c}}(m_{\gamma\gamma}, \boldsymbol{\theta}^{\mathrm{shape}}_{\mathrm{non-res}})] / N_c(\boldsymbol{\theta}^{\mathrm{yield}}_{\mathrm{non-res}})$$

κ_λ reweighting for ggF HH samples

Common HH procedure: derive the scale factors as a function of κ_λ in **bins of m_{HH}** by performing a linear combination of truth level HH ggF samples generated at $\kappa_\lambda = 0, 1, 20$.

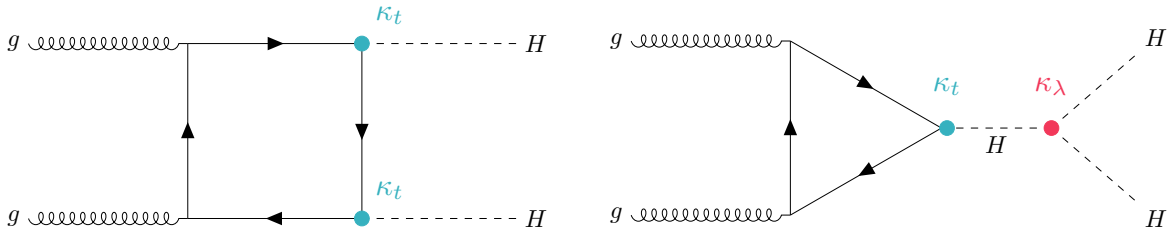

$$\mathcal{A}(\kappa_t, \kappa_\lambda) = \kappa_t^2 \mathcal{A}_1 + \kappa_t \kappa_\lambda \mathcal{A}_2$$

$$\sigma_{\text{ggF}}(pp \to HH) \propto \int \kappa_t^4 \left[|\mathcal{A}_1|^2 + 2\left(\frac{\kappa_\lambda}{\kappa_t}\right) \Re(\mathcal{A}_1^* \mathcal{A}_2) + \left(\frac{\kappa_\lambda}{\kappa_t}\right)^2 |\mathcal{A}_2|^2 \right]$$

$$\begin{aligned}
\sigma(\kappa_t = 1, \kappa_\lambda = 0) &\sim |\mathcal{A}_1|^2 \\
\sigma(\kappa_t = 1, \kappa_\lambda = 1) &\sim |\mathcal{A}_1|^2 + 2\Re \mathcal{A}_1^* \mathcal{A}_2 + |\mathcal{A}_2|^2 \\
\sigma(\kappa_t = 1, \kappa_\lambda = 20) &\sim |\mathcal{A}_1|^2 + 2 \cdot 20 \Re \mathcal{A}_1^* \mathcal{A}_2 + 20^2 |\mathcal{A}_2|^2
\end{aligned}$$

$$\begin{aligned}
\sigma(\kappa_t, \kappa_\lambda) \sim \kappa_t^2 \Bigg[&\left(\kappa_t^2 + \frac{\kappa_\lambda^2}{20} - \frac{399}{380} \kappa_\lambda \kappa_t \right) |S(1,0)|^2 + \left(\frac{40}{38} \kappa_\lambda \kappa_t - \frac{2}{38} \kappa_\lambda^2 \right) |S(1,1)|^2 \\
&+ \left(\frac{\kappa_\lambda^2 - \kappa_\lambda \kappa_t}{380} \right) |S(1,20)|^2 \Bigg]
\end{aligned}$$

HH summary

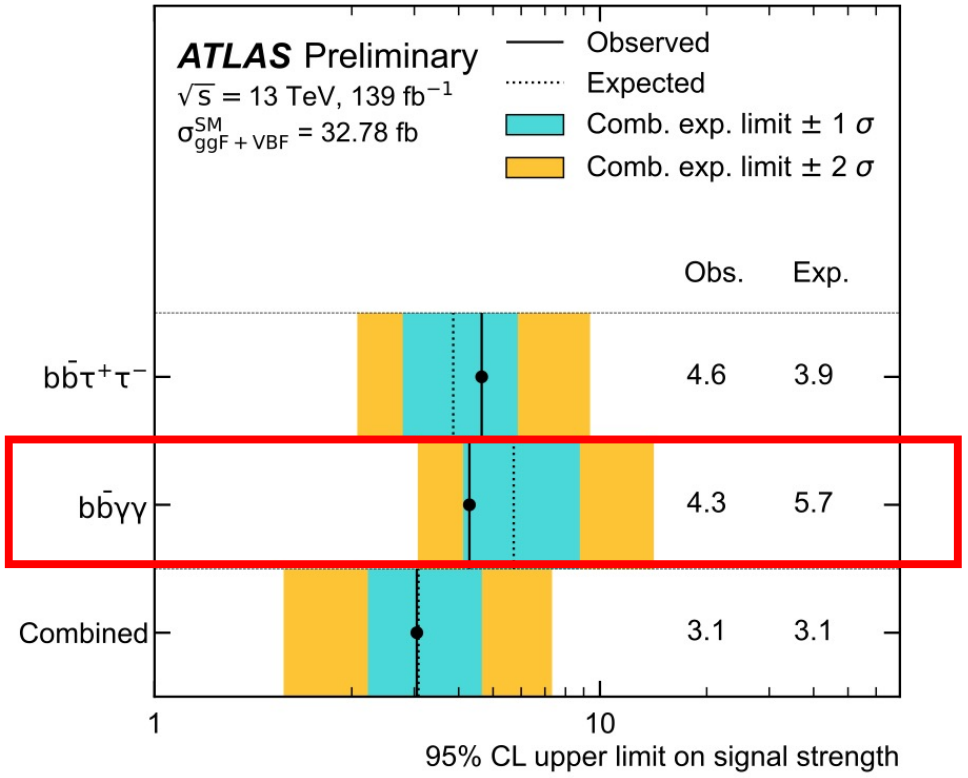

Harmonized mH to 125 GeV

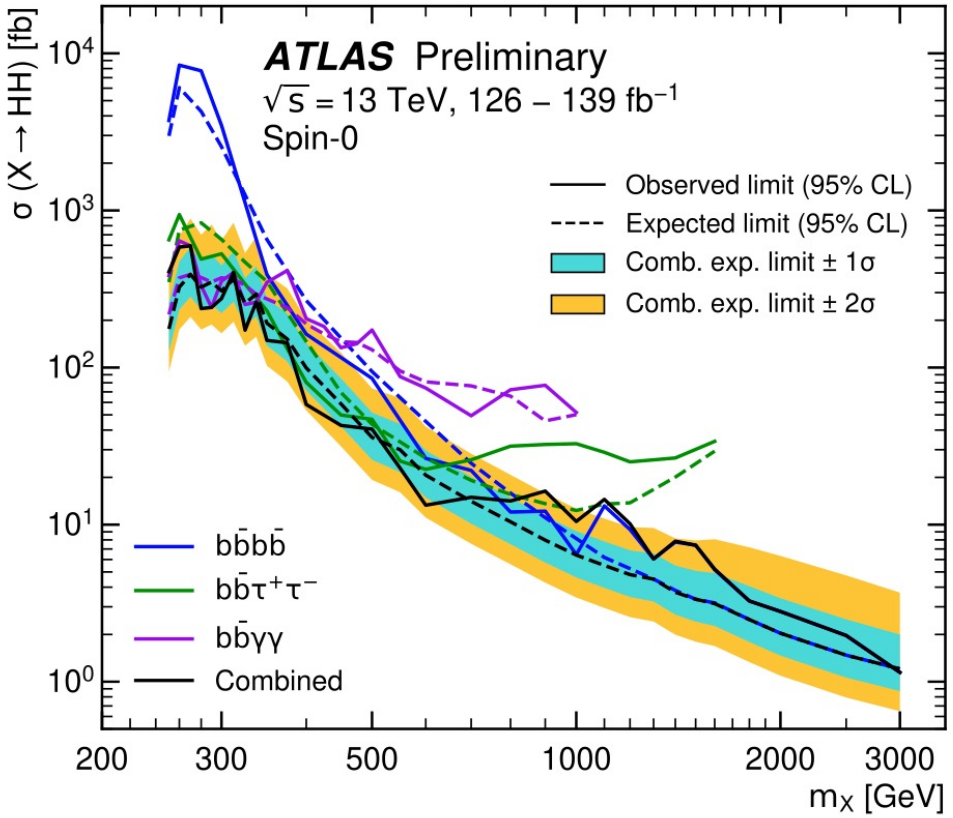

$\gamma\gamma$bb: Good sensitivity at low resonant masses